Magnetic correlations around the Mott transition in the Kagomé lattice Hubbard model

2007 J. Phys.: Condens. Matter 19 145251

(http://iopscience.iop.org/0953-8984/19/14/145251)

IOP PUBLISHING JOURNAL OF PHYSICS: CONDENSED MATTER

J. Phys.: Condens. Matter **19** (2007) 145251 (6pp) doi:10.1088/0953-8984/19/14/145251

Magnetic correlations around the Mott transition in the Kagomé lattice Hubbard model

T Ohashi[1,3], **S-i Suga**[1], **N Kawakami**[1] **and H Tsunetsugu**[2]

[1] Department of Applied Physics, Osaka University, Suita, Osaka 565-0871, Japan
[2] Yukawa Institute for Theoretical Physics, Kyoto University, Kyoto 606-8502, Japan

E-mail: t-ohashi@riken.jp

Received 5 September 2006
Published 23 March 2007
Online at stacks.iop.org/JPhysCM/19/145251

Abstract

We study the magnetic properties around the Mott transition in the Kagomé lattice Hubbard model by using the cellular dynamical mean field theory combined with quantum Monte Carlo simulations. By investigating the **q**-dependence of the susceptibility, we find a dramatic change in the dominant spin fluctuations around the Mott transition. The spin fluctuations in the insulating phase favour down to the lowest temperature a spatial spin configuration in which antiferromagnetic correlations are strong only in one chain direction but almost vanishing in the others.

(Some figures in this article are in colour only in the electronic version)

Geometrical frustration is one of the long-standing problems in spin systems. Recently, frustration effects have also attracted much attention in itinerant electron systems. The observation of heavy fermion behaviour in LiV_2O_4 [1], which has the pyrochlore lattice structure with a corner-sharing network of tetrahedra, has activated theoretical studies of electron correlations with geometrical frustration [2–4]. The discovery of superconductivity in the triangular lattice compound $Na_xCoO_2{\cdot}yH_2O$ [5] and the β-pyrochlore osmate KOs_2O_6 [6] has further stimulated intensive studies of frustrated electron systems. Geometrical frustration has uncovered new aspects of the Mott metal–insulator transition. Among others, a novel quantum liquid ground state was suggested for the insulating phase of the triangular lattice [7], and this may be relevant for frustrated organic materials such as κ-$(ET)_2Cu_2(CN)_3$ [8].

The Kagomé lattice (figure 1) is another prototype of frustrated systems showing many essential properties with the pyrochlore lattice. It is suggested that a correlated electron system on the Kagomé lattice can be an effective model of $Na_xCoO_2{\cdot}yH_2O$ by properly considering anisotropic hopping matrix elements in the cobalt 3d orbitals [9]. The electron system on the Kagomé lattice in the metallic regime was studied recently by using the fluctuation exchange

[3] Present address: Condensed Matter Theory Laboratory, RIKEN, Wako, Saitama 351-0198, Japan.

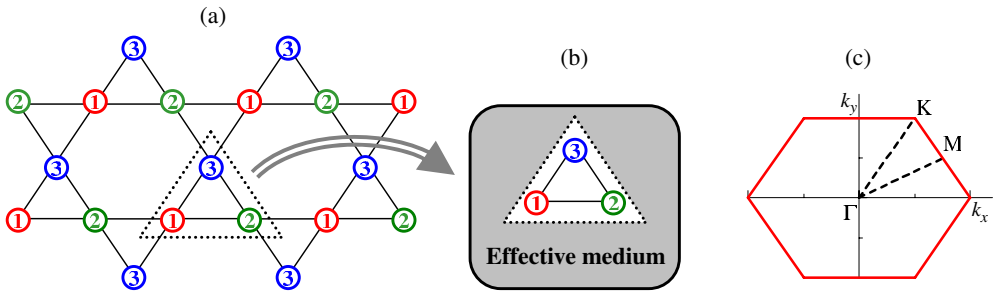

Figure 1. (a) Sketch of the Kagomé lattice and (b) the effective cluster model using three-site cluster CDMFT. (c) First Brillouin zone of the Kagomé lattice.

(FLEX) approximation [10] and quantum Monte Carlo (QMC) method [11], etc [12, 13]. In our recent paper [14], we studied electron correlations in the Kagomé lattice Hubbard model, and found the first-order Mott transition at the Hubbard interaction $U/W \sim 1.37$ (W: band width).

In this paper, we focus on the magnetic properties of the Kagomé lattice Hubbard model. By applying the cellular dynamical mean field theory (CDFMT) [15], we discuss the effects of geometrical frustration around the metal–insulator transition where frustration is stronger than in the weak coupling regime. We consider the standard Hubbard model with nearest-neighbour hopping $t > 0$ on the Kagomé lattice,

$$H = -t \sum_{\langle i,j\rangle,\sigma} c^{\dagger}_{i\sigma} c_{j\sigma} + U \sum_{i} n_{i\uparrow} n_{i\downarrow}, \tag{1}$$

with $n_{i\sigma} = c^{\dagger}_{i\sigma} c_{i\sigma}$, where $c^{\dagger}_{i\sigma}$ ($c_{j\sigma}$) creates (annihilates) an electron with spin σ at the site i. In the following, we use the band width $W = 6t$ as the energy unit. The dynamical mean field theory (DMFT) [16] has given substantial theoretical progress in the field of the Mott transition but it does not incorporate spatially extended correlations. Therefore, in order to take account of geometrical frustration, we use CDMFT, a cluster extension of DMFT [15, 17, 18], which has been applied successfully to frustrated systems such as the Hubbard model on the triangular lattice [19–21].

In CDMFT, the original lattice is regarded as a superlattice consisting of clusters, which is then mapped onto an effective cluster model via a standard DMFT procedure. As shown in figure 1, the Kagomé lattice Hubbard model is mapped onto a three-site cluster coupled to the self-consistently determined medium,

$$S_{\mathrm{eff}} = \int_0^{\beta} \mathrm{d}\tau\, \mathrm{d}\tau' \sum_{\gamma,\delta,\sigma} c^{\dagger}_{\gamma\sigma}(\tau)\, \mathcal{G}^{-1}_{\gamma\delta\sigma}(\tau - \tau')\, c_{\delta\sigma}(\tau') + U \int_0^{\beta} \mathrm{d}\tau \sum_{\gamma} n_{\gamma\uparrow}(\tau)\, n_{\gamma\downarrow}(\tau). \tag{2}$$

Given the Green's function for the effective medium, $\hat{\mathcal{G}}_{\sigma}$, we can compute the cluster Green's function $\hat{G}_{\sigma}$ and the cluster self-energy $\hat{\Sigma}_{\sigma}$ by solving the effective cluster model with the QMC method [22]. Here, $\hat{\mathcal{G}}_{\sigma}$, $\hat{G}_{\sigma}$, and $\hat{\Sigma}_{\sigma}$ are described by 3×3 matrices. The effective medium $\hat{\mathcal{G}}_{\sigma}$ is then computed via the Dyson equation,

$$\hat{\mathcal{G}}^{-1}_{\sigma}(\omega) = \left[\sum_{\mathbf{k}} \hat{g}_{\sigma}(\mathbf{k} : \omega)\right]^{-1} + \hat{\Sigma}_{\sigma}(\omega), \tag{3}$$

$$\hat{g}_{\sigma}(\mathbf{k} : \omega) = \left[\omega + \mu - \hat{t}(\mathbf{k}) - \hat{\Sigma}_{\sigma}(\omega)\right]^{-1}, \tag{4}$$

where μ is the chemical potential and $\hat{t}\,(\mathbf{k})$ is the Fourier-transformed hopping matrix for the superlattice,

$$t_{\gamma\delta}\,(\mathbf{k}) = \sum_{i,j} \mathrm{e}^{-\mathbf{k}\cdot(\mathbf{r}_i - \mathbf{r}_j)} t_{\gamma\delta}\,(i,\, j)\,. \tag{5}$$

Here the summation of $\mathbf{k}$ is taken over the reduced Brillouin zone of the superlattice (see figure 1(c)). After 20 iterations of this procedure, numerical convergence is reached. In each iteration, we typically use 10^6 QMC sweeps and Trotter time slices $L = 2W/T$ to reach sufficient computational accuracy. Furthermore, we exploit an interpolation scheme based on a high-frequency expansion of the discrete imaginary-time Green's function obtained by QMC [23] in order to reduce time slice errors.

We now investigate the magnetic correlation around the Mott transition in the Kagomé lattice Hubbard model. We calculate the wavevector dependence of the static susceptibility,

$$\chi_{\gamma\delta}(\mathbf{q}) = \int_0^{1/T} \mathrm{d}\tau \sum_{\mathbf{k},\mathbf{k}'} \left\langle c^{\dagger}_{\mathbf{k}\gamma\uparrow}\,(\tau)\, c_{\mathbf{k}+\mathbf{q}\gamma\downarrow}\,(\tau)\, c^{\dagger}_{\mathbf{k}'+\mathbf{q}\delta\downarrow}\,(0)\, c_{\mathbf{k}'\delta\uparrow}\,(0) \right\rangle, \tag{6}$$

where $\gamma, \delta = 1, 2, 3$ denote the site indices in the unit cell. We employ the standard procedure in DMFT to calculate $\chi_{\gamma\delta}(\mathbf{q})$ [16], which includes nearest-neighbour correlations as well as on-site correlations. In order to obtain $\chi_{\gamma\delta}(\mathbf{q})$, we first calculate the two-particle Green's function in the effective cluster model (2),

$$\begin{aligned} C_{\gamma\delta}\,(\mathrm{i}\omega_l, \mathrm{i}\omega_m) = T \int_0^{\beta}\int_0^{\beta}\int_0^{\beta}\int_0^{\beta} \mathrm{d}\tau_1\, \mathrm{d}\tau_2\, \mathrm{d}\tau_3\, \mathrm{d}\tau_4 \\ \times \mathrm{e}^{-\mathrm{i}\omega_l(\tau_1-\tau_2)} \mathrm{e}^{-\mathrm{i}\omega_m(\tau_3-\tau_4)} C_{\gamma\delta}\,(\tau_1, \tau_2, \tau_3, \tau_4)\,, \end{aligned} \tag{7}$$

$$C_{\gamma\delta}\,(\tau_1, \tau_2, \tau_3, \tau_4) = \left\langle \mathrm{T}_\tau c^{\dagger}_{\gamma\uparrow}\,(\tau_1)\, c_{\gamma\downarrow}\,(\tau_2)\, c^{\dagger}_{\delta\downarrow}\,(\tau_3)\, c_{\delta\uparrow}\,(\tau_4) \right\rangle, \tag{8}$$

and extract the vertex function $\Gamma_{\gamma\delta}\,(\mathrm{i}\omega_l, \mathrm{i}\omega_m)$ via the Bethe–Salpeter equation,

$$\hat{\Gamma} = \hat{C^0}^{-1} - \hat{C}^{-1}, \tag{9}$$

where C^0 is the bare two-particle Green's function,

$$C^0_{\gamma\delta}(\mathrm{i}\omega_l) = -\frac{1}{T}\left[\sum_{\mathbf{k}} g_{\gamma\delta\downarrow}\,(\mathbf{k} : \mathrm{i}\omega_l)\right]\left[\sum_{\mathbf{k}} g_{\delta\gamma\uparrow}\,(\mathbf{k} : \mathrm{i}\omega_l)\right]. \tag{10}$$

On the other hand, the bare $\mathbf{q}$-dependent Green's function in the lattice system is calculated by

$$C^0_{\gamma\delta}(\mathbf{q} : \mathrm{i}\omega_l) = -\frac{1}{T}\sum_{\mathbf{k}} g_{\gamma\delta\downarrow}\,(\mathbf{k}+\mathbf{q} : \mathrm{i}\omega_l)\, g_{\gamma\delta\uparrow}\,(\mathbf{k} : \mathrm{i}\omega_l)\,. \tag{11}$$

By using equations (9) and (11), we can compute the lattice $\mathbf{q}$-dependent Green's function,

$$\hat{C}\,(\mathbf{q}) = \left[\hat{C^0}\,(\mathbf{q})^{-1} - \hat{\Gamma}\right]^{-1}. \tag{12}$$

Taking account of the phase factor, we finally obtain the $\mathbf{q}$-dependent susceptibility,

$$\chi_{\gamma\delta}(\mathbf{q}) = T^2 \sum_{l,m} C_{\gamma\delta}\,(\mathbf{q} : \mathrm{i}\omega_l, \mathrm{i}\omega_m)\, \mathrm{e}^{-\mathrm{i}\mathbf{q}\cdot(\mathbf{r}_\gamma - \mathbf{r}_\delta)}. \tag{13}$$

It is convenient to introduce $\chi_m(\mathbf{q})$ for three normal modes ($m = 1, 2, 3$) by diagonalizing the 3×3 matrix $\chi_{\gamma\delta}(\mathbf{q})$. In the upper panels of figure 2, we show the three eigenmodes of the susceptibility at $T/W = 1/30$ for several values of interaction strength U/W. In the noninteracting case, the largest eigenvalue of the susceptibility $\chi_1(\mathbf{q})$ takes a maximum at six points in the Brillouin zone, the second largest one, $\chi_2(\mathbf{q})$, has a maximum at $\mathbf{q} = (0, 0)$, and

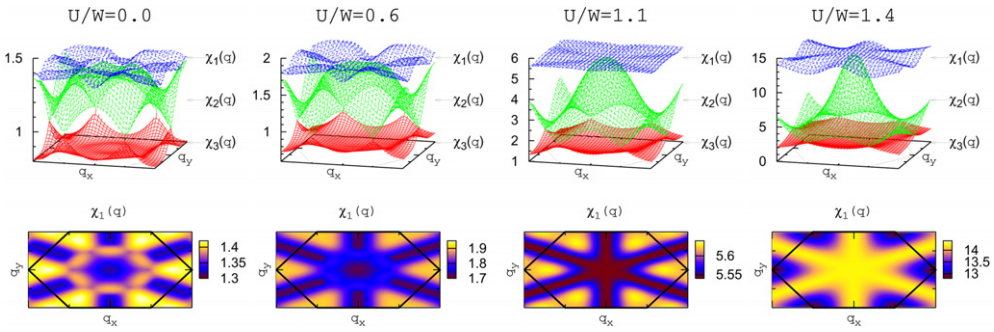

Figure 2. The wavevector dependence of the static susceptibility $\chi_m(\mathbf{q})$ for several values of U/W at $T/W = 1/30$. The three-dimensional plots of $\chi_m(\mathbf{q})$ are shown in the upper panels, from top to bottom, $m = 1, 2, 3$. The two-dimensional plots in the lower panels show the dominant mode of the susceptibility $\chi_1(\mathbf{q})$ in the upper panels. Hexagons in figures denote the first Brillouin zone, as shown figure 1(c).

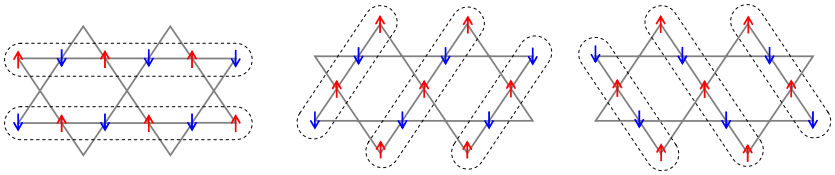

Figure 3. The enhanced spin correlations in the insulating phase $U/W = 1.4$ at $T/W = 1/30$.

the smallest one, $\chi_1(\mathbf{q})$, takes maxima at the corners of the Brillouin zone. As U/W increases, localized moments are formed and the susceptibility is enhanced, as expected. In particular, the $\mathbf{q} = (0, 0)$ peak of $\chi_2(\mathbf{q})$ becomes strongly enhanced, which is consistent with the previous QMC study [11]. On the other hand, the dominant mode of the susceptibility $\chi_1(\mathbf{q})$ shows only weak $\mathbf{q}$-dependence. As U/W increases, $\chi_1(\mathbf{q})$ is enhanced not only at the six points mentioned above but also on the lines passing through Γ and M points, so that the $\mathbf{q}$-dependence of the susceptibility gets suppressed and becomes much weaker at $U/W = 1.1$ than in the noninteracting case. This behaviour is consistent with the previous FLEX calculation in the weak coupling regime [10]. We confirm that the feature of the suppressed $\mathbf{q}$-dependence of the dominant magnetic mode due to geometrical frustration persists up to a fairly large-U region.

We further find notable results in the insulating phase. The Mott metal–insulator transition occurs at $U/W \sim 1.37$ [14]. As shown in the lower panels of figure 2, once the system enters the insulating phase, the $\mathbf{q}$-dependence of $\chi_1(\mathbf{q})$ dramatically changes its character due to the enhancement of short-range antiferromagnetic (AF) correlations [14]. At $U/W = 1.4$, the susceptibility takes the maximum value along the three lines in $\mathbf{q}$ space instead of the six points in the weak coupling regime. Furthermore, by investigating the eigenvectors of $\chi_1(\mathbf{q})$, we find that two spins in the unit cell are antiferromagnetically coupled but the other spin is free. Therefore, at these temperatures, the enhanced spin fluctuations favour a spatial spin configuration in which one-dimensional (1D) AF-correlated spin chains are independently formed in three distinct directions. The three types of enhanced spin correlations are illustrated in figure 3. This spin correlation is one of the naturally expected spin correlation on the Kagomé lattice, because it stabilizes antiferromagnetic configurations in one direction, which is more stable than the naively expected spin configuration having a singlet pair and a free spin in each cluster. These 1D correlations in the finite-T Mott insulating phase are different from the results

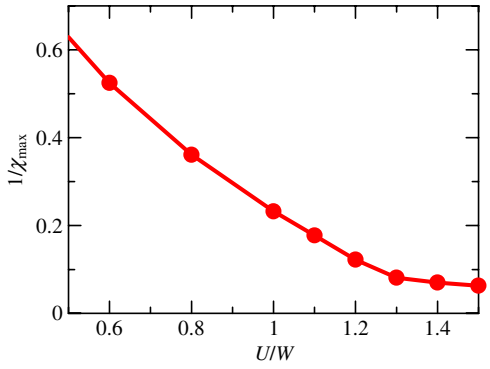

Figure 4. The inverse of the maximum susceptibility, $1/\chi_{max}$, as a function of U/W at $T/W = 1/30$.

for the Heisenberg model on the Kagomé lattice with the nearest-neighbour exchange obtained by both classical and semi-classical approximations [24, 25], but are similar to the $\mathbf{q} = 0$ structure predicted for the classical Heisenberg model with a further neighbour exchange [24]. The essential difference from [24] is that there is almost no correlation between the different chains in our results for the Hubbard model. It remains an interesting problem to compare the q-dependence of the susceptibility in the large-U and low-T regime with the results for the Heisenberg model.

Finally, we show the maximum value of the susceptibility χ_{max} as a function of U/W in figure 4. As U/W increases towards the Mott transition point, $1/\chi_{max}$ decreases almost linearly, as expected. When U/W is further increased and the system enters the insulating phase, the spin correlation changes into the 1D spin correlation, as discussed above, and then χ_{max} saturates. Therefore, we find no evidence of real instability to 1D ordering in the present calculation. However, such enhanced spin fluctuations affect the low-energy dynamics in the insulating phase [14].

In summary, we have studied the magnetic properties around the Mott transition in the Kagomé lattice Hubbard model by means of CDMFT combined with QMC. We have investigated the **q**-dependence of the susceptibility, and obtained results that are consistent with the previous studies: the second-largest eigenmode of the susceptibility shows a strong **q**-dependence, taking a maximum at $\mathbf{q} = (0, 0)$, and the **q**-dependence of the maximum eigenmode of the susceptibility becomes suppressed as U increases in the metallic phase. We also find a dramatic change in the dominant spin fluctuations around the Mott transition. The spin fluctuations in the insulating phase favour a novel spatial spin configuration in which 1D AF-correlated spin chains are independently formed in three distinct directions. Although the spin liquid state or other nonmagnetic ordered states may be stabilized at zero temperature [26], the enhanced 1D spin correlations could emerge in the finite-T Mott insulating phase.

Acknowledgements

The authors thank Y Motome, A Koga, and Y Imai for valuable discussions. Part of the numerical computation was performed at the Supercomputer Center at the Institute for Solid State Physics, University of Tokyo and also at the Yukawa Institute for Theoretical Physics, Kyoto University. This work was partly supported by Grant-in-Aid for Scientific Research (No. 16540313) and for Scientific Research on Priority Areas (Nos 17071011 and 18043017) from Ministry of Education, Culture, Sports, Science and Technology of Japan.

References

[1] Kondo S *et al* 1997 *Phys. Rev. Lett.* **78** 3729
[2] Lacroix C 2001 *Can. J. Phys.* **79** 1469
[3] Tsunetsugu H 2002 *J. Phys. Soc. Japan* **71** 1844
[4] Yamashita Y and Ueda K 2003 *Phys. Rev.* B **67** 195107
[5] Takada K *et al* 2003 *Nature* **422** 53
[6] Yonezawa S, Muraoka Y, Matsushita Y and Hiroi Z 2004 *J. Phys.: Condens. Matter* **16** L9
[7] Kashima T and Imada M 2001 *J. Phys. Soc. Japan* **70** 3052
[8] Shimizu Y, Miyagawa K, Kanoda K, Maesato M and Saito G 2003 *Phys. Rev. Lett.* **91** 107001
[9] Koshibae W and Maekawa W 2003 *Phys. Rev. Lett.* **91** 257003
[10] Imai Y, Kawakami N and Tsunetsugu H 2003 *Phys. Rev.* B **68** 195103
[11] Bulut N, Koshibae W and Maekawa S 2005 *Phys. Rev. Lett.* **95** 037001
[12] Läuchli A and Poilblanc D 2004 *Phys. Rev. Lett.* **92** 236404
[13] Indergand M, Laeuchli A, Capponi S and Sigrist M 2006 *Preprint* cond-mat/0603401
[14] Ohashi T, Kawakami N and Tsunetsugu H 2006 *Phys. Rev. Lett.* **97** 066401
[15] Kotliar G, Savrasov S Y, Pálsson G and Biroli G 2001 *Phys. Rev. Lett.* **87** 186401
[16] Georges A, Kotliar G, Krauth W and Rozenberg M J 1996 *Rev. Mod. Phys.* **68** 13
[17] Biroli G, Parcollet O and Kotliar G 2004 *Phys. Rev.* B **69** 205108
[18] Maier T, Jarrell M, Pruschke T and Hettler M H 2005 *Rev. Mod. Phys.* **77** 1027
[19] Parcollet O, Biroli G and Kotliar G 2004 *Phys. Rev. Lett.* **92** 226402
[20] Civelli M, Capone M, Kancharla S S, Parcollet O and Kotliar G 2005 *Phys. Rev. Lett.* **95** 106402
[21] Kyung B and Tremblay A-M S 2006 *Phys. Rev. Lett.* **97** 046402
[22] Hirsch J E and Fye R M 1986 *Phys. Rev. Lett.* **56** 2521
[23] Oudovenko V S and Kotliar G 2002 *Phys. Rev.* B **65** 075102
[24] Harris A B, Kallin C and Berlinsky A J 1992 *Phys. Rev.* B **45** 2899
[25] Chubukov A 1992 *Phys. Rev. Lett.* **69** 832
[26] Misguich G and Lhuillier C 2004 *Frustrated Spin Systems* ed H T Diep (Singapore: World Scientific) and references therein